DOI: 10.1534/genetics.109.113670

Identification of Genes Affecting Wing Patterning Through a Loss-of-Function Mutagenesis Screen and Characterization of *med15* Function During Wing Development

Ana Terriente-Félix,[1] Ana López-Varea and Jose F. de Celis[2]

Centro de Biología Molecular "Severo Ochoa," Consejo Superior de Investigaciones Científicas and Universidad Autónoma de Madrid, Cantoblanco, Madrid 28049, Spain

Manuscript received December 29, 2009
Accepted for publication March 4, 2010

ABSTRACT

The development of the *Drosophila melanogaster* wing depends on the correct regulation of cell survival, growth, proliferation, differentiation, and pattern formation. These processes, and the genes controlling then, are common to the development of epithelia in many different organisms. To identify additional genes contributing to wing development we have carried out a genetic screen in mosaic wings carrying clones of homozygous mutant cells. We obtained 12 complementation groups corresponding to genes with a proven role in wing formation such as *smoothened*, *thick veins*, *mothers against dpp*, *expanded*, and *fat* and 71 new complementation groups affecting the pattern of veins and the size of wing. We mapped one of these groups to the *mediator15* gene (*med15*), a component of the Mediator complex. We show that Med15 and other members of the Mediator complex are required, among other processes, for the transcription of *decapentaplegic* target genes.

THE Drosophila wing imaginal disc is an epithelium of undifferentiated cells that grows and becomes patterned during the larval period and that differentiates the fly wing during the pupal stage (Cohen 1993). The patterning of the wing disc involves the activities of several signaling pathways that act in collaboration with sequence-specific transcription factors to define cell fates (reviewed in de Celis 2003). First, the wing blade is specified as a domain of *vestigial* (*vg*) expression in the distal region of the wing disc by the activities of the Wingless (Wg), Epithermal growth factor receptor/Ras (EGFR/RAS), and Decapenteplegic (Dpp) signaling pathways (Williams *et al.* 1991; Kim *et al.* 1996). Later in development, the wing blade is subdivided into provein and intervein regions by the activities of the Dpp and Hedgehog (Hh) signaling pathways (reviewed in Bier 2000; de Celis 2003). Adjacent proveins are separated by broader "intervein" regions that correspond to domains of expression of the transcription factor Blistered (Bs) (Fristrom *et al.* 1994; Montagne *et al.* 1996; Roch *et al.* 1998). The expressions of vein-specific transcription factors in the proveins and Bs in the interveins regulate the expression of *rhomboid* (*rho*), leading to the generation of high levels of EGFR/RAS activity in these cells and to their differentiation as veins during pupal development (reviewed in Bier 2000; de Celis 2003).

Genetic screens have been instrumental in the identification of genes involved in the generation of a wing with a characteristic size and pattern of veins. In general, the imaginal discs are best suited for gain-of-function screens and for screenings carried out in sensitized genetic backgrounds, because these experiments can be done in heterozygous individuals. More conventional screens aiming to identify genes on the basis of their loss-of-function phenotype have not being frequently used, as most of the mutations of interest are likely to be homozygous lethal. These mutations can be identified only in mosaic animals, which with some exceptions (Garcia-Bellido and Dapena 1974) has prevented these experiments until the adoption of the FRT/FLP method to induce mitotic recombination (Xu and Harrison 1994). Since then, several loss-of-function screens have being reported in adult flies, using a heat-shock (*hs*) promoter to drive the expression of the FLP enzyme (Walsh and Brown 1998) or directing the expression of FLP to a particular domain of expression in the eye disc (Xu *et al.* 1995). In these cases, the mutations are identified in heterozygous animals bearing patches of homozygous cells induced by recombination between homologous FRT elements. These experiments allow the identification of genes required for imaginal development whose mutations are homozygous lethal.

Supporting information is available online at http://www.genetics.org/cgi/content/full/genetics.109.113670/DC1.

[1]*Present address:* Department of Zoology, University of Cambridge, Cambridge CB2 3EJ, United Kingdom.

[2]*Corresponding author:* Centro de Biología Molecular "Severo Ochoa," Consejo Superior de Investigaciones Científicas and Universidad Autónoma de Madrid, Cantoblanco, Madrid 28049, Spain.
E-mail: jfdecelis@cbm.uam.es

We have adopted a variation of this method by combining FRT/FLP mitotic recombination with a source of FLP expressed in a broad domain of the wing blade and used a *Minute* mutation (*M*) to increase the proportion of homozygous mutants cells that otherwise might be eliminated due to their reduced viability. In our experimental setting, we induced mutations using ethyl nitrous urea (ENU) and selected heterozygous flies with a wing phenotype caused by the presence of M^+ clones in the domain of expression of *spalt* (*sal*). In this experiment, carried out in an F_1 generation, we isolated 140 mutations affecting the development of the wing. These mutants were classified in phenotypic classes, grouped in complementation groups, and then mapped to chromosomal intervals by complementation with a set of deficiencies covering 83% of the 2L arm. Among the complementation groups identified, 12 correspond to genes already known for their involvement in wing development, such as *smoothened* (*smo*), *net*, *thickveins* (*tkv*), *mothers against dpp* (*mad*), *Star* (*S*), *expanded* (*ex*), *Suppressor of Hairless* [*Su(H)*], *cdc2*, *echinoid* (*ed*), *Protein kinase A* (*PKA*), *kuzbanian* (*kuz*), and *fat* (*ft*), 16 are new complementation groups composed of at least two mutants, and 55 mutations appear to correspond to single alleles. We present here this screen and the mapping and characterization of one complementation group that corresponds to *med15*, a gene encoding a component of the Mediator complex (Lewis and Reinberg 2003; Guglielmi *et al.* 2004). The Mediator complex (Med) is conserved from yeast to humans and promotes the interaction of the RNApol-II with sequence-specific transcription factors (Kwon *et al.* 1999; Naar *et al.* 2001). We show that Med15 and other members of the Med complex are required, among other processes, for the transcription of *dpp* target genes. Interestingly, the *med15* homolog in *Xenopus laevis*, ARC105, regulates specifically the expression of Smad3/4 and Smad2/4 target genes (Kato *et al.* 2002), suggesting a high degree of conservation of Med15-specific functions during evolution.

MATERIALS AND METHODS

Drosophila stocks: Flies were cultured on standard media and crosses were carried out at 25° unless otherwise stated. We used the following stocks: *hh-Gal4* (Calleja *et al.* 1996), sal^{EPv}-*Gal4* and *638-Gal4* (Cruz *et al.* 2009), *UAS-tauGFP* (Ito *et al.* 1997), *UAS-FLP* (Duffy *et al.* 1998), nub^1, *Df(2L)vg*, ap^{HGO35}, smo^3 (Chen and Struhl 1996), pka^{B3} (Li *et al.* 1995), *TE35BC-GW24* (*su(H)*) (Morel and Schweisguth 2000), kuz^{1405} (Sotillos *et al.* 1997), Sos^{34Ea-6} (Rogge *et al.* 1991), $spen^5$ (Kuang *et al.* 2000), spi^1 (Freeman 1994), tkv^{A12} (Nellen *et al.* 1994), *Df(2L)ed-dp* (a gift from S. Campuzano), net^1 (Brentrup *et al.* 2000), aop^1 (Rogge *et al.* 1995), fat^{l18} (Mahoney *et al.* 1991), $cass^{2L-5}$ (Prout *et al.* 1997), *Df(2L)LamB1* (Urbano *et al.* 2009), $cdc2^{B47}$ (Clegg *et al.* 1993), dpp^{d12} (St. Johnston *et al.* 1990), $Df(2L)wg^{CX3}$ (Baker 1987), ex^1 (Boedigheimer *et al.* 1993), lgl^4 (a gift from A. Pérez), $P\{lacZ\}bib^{4163}$ (Hao *et al.* 2003), the PyggyBac insertions *d00080* and *f06555* (Parks *et al.* 2004), and interference RNA lines against the genes *med15* (NIG-Fly 4184R-4), *med30* (VDRC 32459), *med20* (NIG-Fly 18780R-3), med27 (NIG-Fly 1245R-1), *med19* (NIG-Fly 5546R-1), *med10* (NIG-Fly 5057R-1), *med12/kto* (NIG-Fly 8491R-2), *med16* (NIG-Fly 5465R-1), and *med25* (NIG-Fly12254R-1).

Generation of mitotic recombination clones: We induced mitotic recombination by Flipase (*FLP*) at 48–72 hr after egg laying (AEL) in larvae of the following genotypes:

hsFLP1.22 f^{36a}*; M(2)z P[f+]30C FRT40A/mut al dp b pr FRT40A* (*f* M^+ clones)
hsFLP1.22 f^{36a}*; ck P[f+]30C FRT40A/mut al dp b pr FRT40A* (*ck*/*f* twin clones)
sal^{EPv}*-Gal4* f^{36a}*; M(2)z P[f+] FRT4A/mut FRT40A; UAS-FLP/+*
sal^{EPv}*-Gal4; M(2)z P[f+] FRT40A/mut FRT40A; UAS-FLP/+*
w; M(2)z P[f+]30C FRT40A/mut al dp b pr FRT40A; hh-Gal4/UAS-FLP
638-Gal4; M(2)z P[f+] FRT40A/mut FRT40A; UAS-FLP/+
sal^{EPv}*-Gal4; M(2)z P{arm-lacZ} FRT40A/mut FRT40A; UAS-FLP/+*
638-Gal4; M(2)z P{arm-lacZ} FRT40A/mut FRT40A; UAS-FLP/+.

The sal^{EPv}*-Gal4; al dp b FRT40A/FRT40A M(2)zFRT40A; UAS-FLP/+* wing disc contains homozygous *al dp b* M+ clones in the wing blade. The number of clones and their sizes increase during the third larval instar. We find clones covering ~80% of the wing central domain in the corresponding adult wings. The wing blade region of *638-Gal4;al dp b FRT40A/FRT40AA M(2)zFRT40A; UAS-FLP/+* discs became entirely mutant in third instar larvae. The *dp* phenotype is apparent only in mosaic wings generated using the *638-Gal4* driver, suggesting that it is necessary for a large fraction of *dp* cells for this phenotype to develop. The presence of the *dp* allele does not interfere with phenotypes affecting pattern and/or size.

ENU treatment: Groups of 50 *w; al dp b pr FRT40A; UAS-FLP* isogenic males 3 days old were first left starving for 4 hr and then fed during 24 hr with 0.29 mg/ml ENU in a sucrose solution. This concentration is estimated to cause one mutation per chromosomal arm (Ashburner 1989). Treated males were crossed with 100 *salPE-Gal4; M(2)z FRT40A/CyO* females and discarded after 3 days.

Complementation assays: Mutants showing a similar phenotype in mosaic wings were crossed with each other, and mutations whose combination gave lethality or a visible wing phenotype were considered members of the same complementation group. We also used in these crosses the following alleles of genes localized in the 2L arm: smo^1, pka^{B3}, big^{lacZ}, *TE35BC-GW24* (*su(H)*), kuz^{14C5}, SOS^{34Ea-b}, $spen^5$, $S^{PZ05671}$, spi^{EC2}, mad^{B1}, tkv^{A12}, *Df(2L)ed-dp*, net^{l1}, aop^1, fat^{l18}, $cass^{2L-5}$, *Df(2L)LamB1*, $cdc2^{B47}$, dpp^{d5}, wg^{CX3}, ex^1, and lgl^4.

Complementation with deficiencies: To map the mutants to a cytological position, they were crossed with a group of deficiencies covering the 2L chromosomal arm. The deficiencies utilized were as follows: *Df(2L)net-PMF* (BL3638), *Df(2L)al* (BL3548), *Df(2L)ast2* (BL3084), *Df(2L)BSC37* (BL7144), *Df(2L)dppd14* (BL6648), *Df(2L)C144* (BL90), *Df(2L)JS17* (BL1567), *Df(2L)BSC28* (BL6875), *Df(2L)BSC31* (BL6965), *Df(2L)drm-P2* (BL6507), *Df(2L) ed1* (BL5330), *Df(2L)ED250* (BL9270), *Df(2L)BSC109* (BL8674), *Df(2L)Exel6011* (BL7497), *Df(2L)cl-h3* (BL781), *Df(2L)E110* (BL490), *Df(2L)BSC6* (BL6338), *Df(2L)BSC7* (BL6374), *Df(2L)spdj2* (BL2414), *Df(2L)XE-2750* (BL4955), *Df(2L)TE29Aa-11* (BL179), *Df(2L)N22-14* (BL2892), *Df(2L)s1402* (BL556), *Df(2L)Mdh* (BL1045), *Df(2L)BSC32* (BL7142), *Df(2L) FCK-20* (BL5869), *Df(2L)Prl* (BL3079), *Df(2L)prd1.7* (BL3344), *Df(2L)BSC30* (BL6999), *Df(2L)b87e25* (BL3138), *Df(2L)TE35BC-24* (BL3588), *Df(2L)r10* (BL1491), *Df(2L)cact 255rv64* (BL2583), *Df(2L)TW137* (BL420), *Df(2L)TW50* (BL3189), and *Df(2L)TW161* (BL167). We first crossed one allele of each complementation group and all

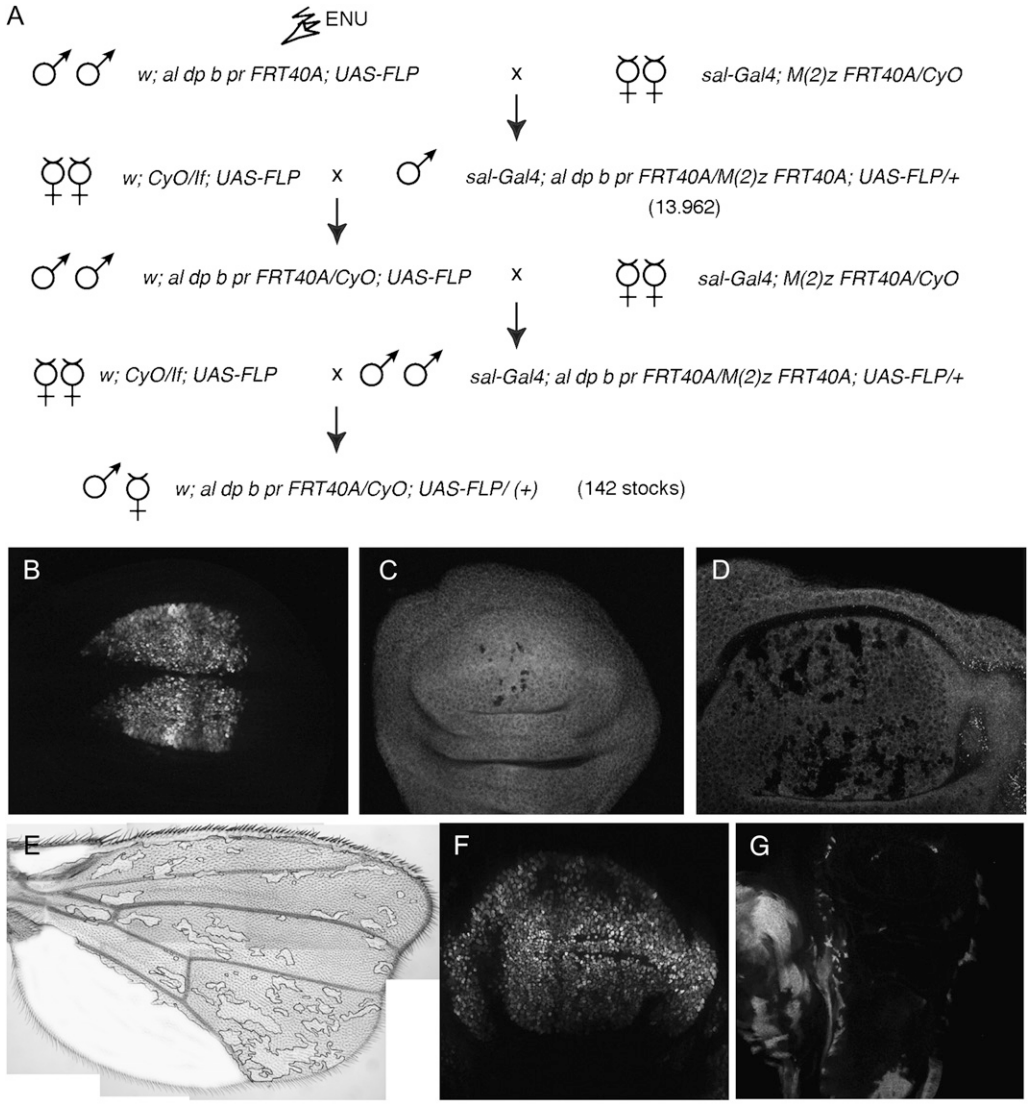

FIGURE 1.—Crosses and Gal4 lines used to generate homozygous mutant wings in heterozygous flies. (A) Chromosomes and genetic crosses used to generate mosaic flies. Males of *w; al dp b pr FRT40A; UAS-FLP* genotype were treated with ENU and crossed in groups of 50 with *sal^{EPv}-Gal4; M(2)Z FRT40A/CyO* females (first row). The *sal-Gal4; M(2)Z FRT40A/al dp b pr FRT40A; UAS-FLP/+* male progeny (13,962 males, second row) was screened for wing phenotypes. Selected males were crossed with w; CyO/If; UAS-FLP females, and the male progeny of w; *al dp b pr FRT40A/CyO; UAS-FLP* genotype were crossed with *sal^{EPv}-Gal4; M(2)Z FRT40A/CyO* females. We established stable w; *al dp b pr FRT40A;UAS-FLP/+* stocks when the original phenotype was found in the progeny of this last cross (142 cases). (B) Expression of GFP in the wing blade region of the *sal^{EPv}-Gal4/UAS-GFP* wing disc. (C and D) Early (C) and late (D) third instar wing discs of *sal^{EPv}-Gal4; M(2)Z FRT40A tubGFP/al dp b pr FRT40A; UAS-FLP/+* genotype, showing the clones as black spots. (E) Adult wing of *f^{36a} sal^{EPv}-Gal4; M(2)Z FRT40A Pf^{+} 30C/al dp b pr FRT40A; UAS-FLP/+* genotype, showing the area not covered by *forked* clones in white. (F) Third instar wing disc showing the expression of the *638-Gal4* line (*638-Gal4/UAS-GFP*). (G) Third instar wing disc of *638-Gal4; M(2)Z FRT40A tubGFP/al dp b pr FRT40A; UAS-FLP/+* genotype. Most of the wing blade is composed of *al dp b pr FRT40A* homozygous cells (shown in black).

single mutants with these deficiencies. Subsequently, all mutations belonging to each complementation group were crossed with the corresponding deficiencies. Due to the presence of associated lethals in the treated chromosomes, we can be confident of the mapping data only for complementation groups with more than one allele (see Table S1 and Table S2).

Mapping of the complementation group affecting *med15*: The *77A2* and *133A1* mutants were lethal over *Df(2L)al* and consequently were mapped to the 21B8–C1;21C8–D1 interval. They were then crossed with a group of smaller and molecular mapped deficiencies, *Df(2L)ED5878* (BL9353), *Df(2L)ED19* (BL8901), *Df(2L)BSC16* (BL6608), *Df(2L)BSC106* (BL8672), *Df(2L)BSC107* (BL8673), and *Df(2L)ast4* (BL6115), resulting in lethality in combination with *Df(2L)BSC107*. We then generated a new smaller deficiency by FRT recombination between the PBac insertions *XP(+)d00080* and *WH(+)f06555*, allowing the localization of *77A2* and *133A1* to an interval including eight genes. Finally, both alleles failed to complement with the PBac insertion *MED15^{f04180}*. To confirm that these mutations are *med15* alleles, we amplified and sequenced the genomic region of *med15* from *77A2* and *133A1* embryos using the following primers: med15-1L, TCACACTGTGCT CAGAGAAGAAGA; med15-1R, GTTGCATGGCATTTACGTT; med15-2L, AAATGCCATGCAACAGATGCCT; med15-2R, AAA TGCAATAGCTGCGAAAAA; med15-3L, GATGTGGAGAAGAT GACAAAG; and med15-3R, ACACTTTTTGCCCAGCGTAA.

Immunocytochemistry and *in situ* hybridization: Wings discs were dissected, fixed, and stained as described in DE CELIS (1997). To detect apoptotic cells we used anti-activated Caspase3 (1:50; Cell Signaling), rabbit anti-Sal (1:200; BARRIO and DE CELIS 2004), and rabbit anti-PMad (1:1000; a gift from G. Morata). Secondary antibodies were from Jackson Immunological Laboratories (used at 1/200 dilution). Pictures were taken with an Axioplan 2 Zeiss microscope and confocal images with a Microradiance–Bio-Rad microscope.

RESULTS

We aimed to identify loss-of-function mutations affecting the development of the Drosophila wing. Be-

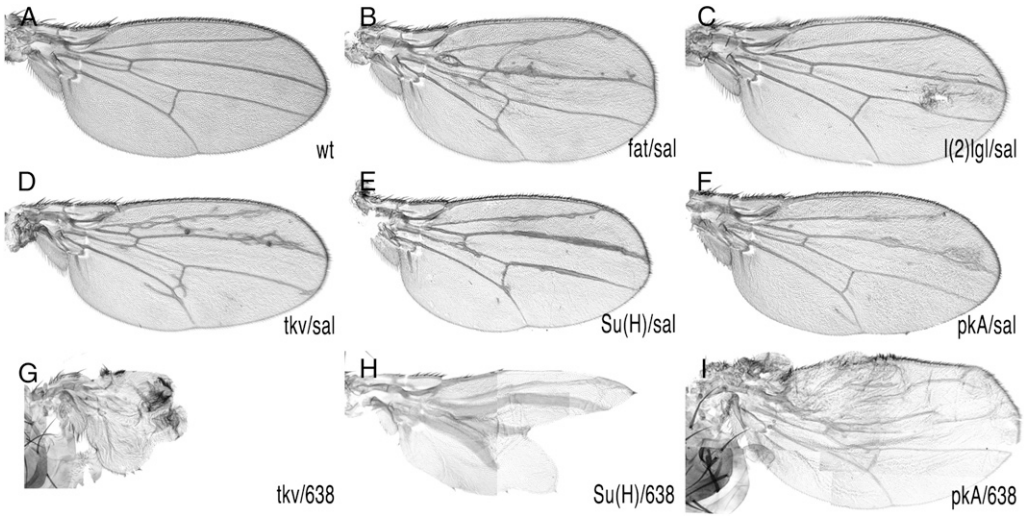

Figure 2.—Mosaic wings of known mutants affecting wing development. (A) Wild-type wing. (B) *sal^{EPv}-Gal4; M(2)Z FRT40A/ fat^{18} FRT40A; UAS-FLP/+* (*fat/sal*). (C) *sal^{EPv}-Gal4; M(2)Z FRT40A/ l(2)gl^{4} FRT40A; UAS-FLP/+* [*l(2)gl/sal*]. (D) *sal^{EPv}-Gal4; M(2)Z FRT40A/tkv^{a12} FRT40A; UAS-FLP/+* (*tkv/sal*). (E) *sal^{EPv}-Gal4; M(2)Z FRT40A/ TE35BC-GW24 FRT40A; UAS-FLP/+* [*Su(H)/sal*]. (F) *sal^{EPv}-Gal4; M(2)Z FRT40A/ PKA^{B3} FRT40A; UAS-FLP/+* (*PKA/sal*). (G) *638-Gal4; M(2)Z FRT40A/ tkv^{a12} FRT40A; UAS-FLP/+* (*tkv/638*). (H) *638-Gal4; M(2)Z FRT40A/ TE35BC-GW24 FRT40A; UAS-FLP/+* [*Su(H)/638*]. (I) *638-Gal4; M(2)Z FRT40A/ PKA^{B3} FRT40A; UAS-FLP/+* (*PKA/638*). Note that the phenotypes involving the Gal4 driver *638-Gal4* are much stronger than those generated with *sal-Gal4*.

cause most mutants are expected to be homozygous lethal (Ripoll and Garcia-Bellido 1979), we developed a method allowing the generation of viable and fertile heterozygous F_1 animals bearing clones of cells homozygous for newly induced mutants in the wing blade (Figure 1A). In *sal^{EPv}-Gal4; al dp b pr mut FRT40A/FRT40A M(2)z; UAS-FLP/+* males, the expression of FLP in the wing blade driven by *sal^{EPv}-Gal4* during the third larval instar (Figure 1B) induces FRT-mediated mitotic recombination in the 2L and results in the generation of cells homozygous for the *al dp b pr mut FRT40A* chromosomal arm. These cells also lose the *Minute* mutation [*M(2)z*] and grow to occupy large extents of the central domain of the wing blade (Figure 1, *C–E*). We also used *638-Gal4* to generate mosaic wings. *638-Gal4* expression starts during the second larval instar and occurs in all wing cells (not shown and Figure 1F). In this case the entire wing blade and hinge became homozygous (Figure 1G). To estimate the visibility of phenotypes and the viability and fertility of heterozygous animals with mosaic wings, we induced clones of cells homozygous for mutations in genes whose roles in wing formation are well established. We used lethal alleles of *fat* (*ft*), *lethal (2) giant larvae* [*l(2)gl*], *thick veins* (*tkv*), *Suppressor of Hairless* [*Su(H)*], and *Protein kinase A* (*PkA*). In all cases and for both drivers, *sal^{EPv}-Gal4* and *638-Gal4*, the resulting mosaic animals display wing phenotypes that were easy to identify under the dissecting microscope (Figure 2). The phenotypes of combinations involving *638-Gal4* were always stronger than those of the corresponding combinations using *sal^{EPv}-Gal4* (compare Figure 2D with 2G, 2E with 2H, and 2F with 2I). However, the viability of *638-Gal4* combinations was poor, and in many cases adult animals can be recovered only as escapers. For these reasons we used the *sal^{EPv}-Gal4* driver for the screen and the *638-Gal4* driver to analyze the phenotype of homozygous mutant wings.

Establishment of complementation groups: We scored ~14,000 males of the *sal^{EPv}-Gal4; al dp b pr mut FRT40A/ FRT40A M(2)z; UAS-FLP/+* genotype, where *mut* means a recessive mutation induced in 2L. From the F_1 males with abnormal wings we established 140 *w; al dp b pr mut FRT40A/CyO* stocks, and subsequently we used them to generate mosaic animals in which mitotic recombination is driven in the *638-Gal4* domain of expression. We grouped these alleles using the phenotypes of the combinations involving the *sal^{EPv}-Gal4* and *638-Gal4* drivers and then crossed all the mutants in each group by each other to establish putative complementation groups. One member of each complementation group was crossed with alleles of known genes showing a similar phenotype in mosaics. The result of this analysis is shown in Table 1 (new complementation groups) and Figure 3A (complementation groups of known genes). As a summary, we identified 83 complementation groups, of which 12 correspond to previously known genes (Figure 3A) and 71 to mutations in other as yet unidentified genes (Figure 3B). The group of "known" genes had the higher number of alleles per complementation group (Figure 3B), whereas of the 71 novel complementation groups only 16 had more than one allele (Table 1 and Figure 3B). Although there is some correlation between the size of the coding region and the number of alleles identified for each known gene (Figure 3A), other aspects of the mutants appear more relevant to determine the probability of their identification.

Phenotypic classes obtained in the screen: The phenotypes of alleles not corresponding to previously known genes were classified in the following groups: (1) mutants affecting primarily the development of the veins, causing the loss of vein stretches, the formation of ectopic veins, or an increase in the thickness of the veins (Figure 4, A–C); (2) mutants affecting the integrity of

TABLE 1

Mutants identified in the screen grouped in phenotypic classes (first column), indicating the different alleles identified ("Alleles" column), the number of alleles included in each complementation group ("No."), the phenotype in the combinations *sal^{EPv}-Gal4/+; FRT40A mut al dp b pr/FRT40A M(2)z; UAS-FLP/+* ("SAL-GAL4") and *638-Gal4/+; FRT40A mut al dp b pr/FRT40A M(2)z; UAS-FLP/+* ("638-GAL4"), and the name of the deficiency they fail to complement ("Def")

Phenotypic class	Alleles	No.	SAL-GAL4	638-GAL4	Def
Loss of veins	MED15	2	−v	+v/−v/+SO	3548
	88A2	1	−s/−v/bs	−v	167
	95C4	1	−v/bs	−v/wm/CD	4955
	106B3	1	−v	+v/−v	—
	128C3	1	−v	−L4	167
Ectopic veins	**kismet**	6	+v/+s	+v/+s	3638
	111B4	1	+v	—	**>2**
	139B	1	+v	+v/+v	490
L3 duplication	93A2, 93A6	1	+v	+v/wm/N	6999
	46B4	1	+L3	+v/+v/wm	**2**
	106D5	1	+v	+v/+v/wm	**>2**
	112B3/147A2	2	+v/CD	+v/wm/−L4	**5330**
Ectopic veins/loss of wing margin	46B5	1	+v	+v	2
	68B	1	wt	+v/wm	—
	92C2	1	+v/bs	wm	6648
	111C6	1	+v	+v/wm	8674
	81C, 108D2, 112D1, 173A2, 184A3	5	+v	+v/wm	6338
	127C3	1	+v	−v/wm	**2**
	130D1	1	+v/+s	−v/−L2/−L5/wm	**>2**
	132A2, 137C2, 146A2	3	+v/bs/+v	+v/wm	6507
	146C,147A1	2	+v/bs	+v/wm	—
	178B	1	+v/+v	+v/wm	420
	185A2	1	+v	+v/+v	2583
	195A	1	+v/bs	+v/wm	**420/3189**
Thicker veins	**20C, 39B2, 190A3**	3	N	N/wm	3548
	50B2	1	+v	N/wm	**2**
	112D7	1	N	N	—
	116C1	1	bs/+s	N	**>2**
Loss of wing margin	**45C5, 149B2**	2	wm	+v/wm	3548
Ectopic veins/loss of wing margin	AT3, 147C2	2	bs	+v/wm	—
	27C2	1	v+	+v/+v/wm	3189
	37C	1	+v	+v/wm	781
	41B	1	+v	+v/wm	**2**
Larger wings	**130C1**	1	+s	+s	**5330**
	111B1	1	bs	+s	—
	21D, 39D3	2	N	+s/+L3	1045
Smaller wings	14B1	1	+v/+v	+v	8674
	24C	1	+v	+v	2414
	29D1	1	+v/bs	+v	—
	31B1, 110B4, 142C3	3	+v	+v/bs	5330
	89B2	1	+v	+v	**3138**
	101B1	1	+v	+v/N	1491
	119D5	1	+v	+v/+v/bs	—
	132A1	1	+v/+SO	+v/bs	**>2**
	149C	1	+v	+v	**>2**
	173B5	1	+v	+v	167
	181B	1	+v	+v/−L2	—
	184E	1	+v	+v	—
Blister	**18C2, 101A, 149C5**	3	bs	+v/bs	3548
	62B1	1	bs	bs	4955
	131B2	1	wt	+v/bs	5330
	179B3	1	bs	bs	7142
	190A1	1	bs	+s	781

(*continued*)

TABLE 1

(Continued)

Phenotypic class	Alleles	No.	SAL-GAL4	638-GAL4	Def
Blister and pattern defects	24A	1	N/CD	+v/N	167
	29A2	1	+v/CD	+v/+L3/CD	7144
	77A, 82A2, 119D2	3	CD	+v/+v/wm	1491
	80B2/80B3	1	N/bs	+v/+v/wm	**2**
	113B1, 136B1	2	+v/−L4/CD	L	**420/3189**
	66B, 127C4	2	bs	+v/+v	—
	89B4	1	+v	+v/+v	2
	96C1	1	bs	L	2583
	110B5	1	bs	+v/+v/wm	167
	136B3, 136B2	1	bs	+v/+v/wm	6965
	157B3	1	+v/bs/CD	+v/+v/wm	**2**
	180A1	1	+v/bs	+v/+v/wm/CD	3189
	78B	1	wt	+v	7144
Cell differentiation	29C2	1	CD	+v/wm/CD	**2**
	52C1, 79A3, 101D, 130D2	4	CD	+v/wm/CD	—
	67A1	1	+v/CD/+v	+v/wm/CD	6999
	75B5	1	+v/CD	+v/bs/CD	**2**
	141C5	1	+v/CD/+v	L	>**2**
Total	**71**	**101**			

Abbreviations in the SAL-GAL4 and 638-GAL4 columns are as follows: −v, loss of veins; +v, ectopic veins; −s, reduced size; +s, larger size; +SO, ectopic sensory organs in the wing blade; bs, loss of dorso-ventral adhesion; N, thicker veins; wm, loss of wing margin; CD, trichome differentiation or planar cell polarity; L, lethal. In some cases individual veins are also indicated. In the "Def" column, 2 and >2 indicate that the corresponding mutation fails to complement two or more than two chromosomal deficiencies, respectively.

the wing margin, causing the loss of wing tissue around the wing margin (Figure 4D) [some of these mutants also affect the distance between the longitudinal veins (Figure 4, E and F)]; (3) mutants affecting mainly the size of the wing with no or only minor effects in the patterning of veins (Figure 5, B and C); (4) mutants affecting the adhesion between the dorsal and ventral wing surfaces (Figure 5, D and E); and (5) mutants affecting the differentiation of trichomes (Figure 5F). Although most mutants can be assigned to one of these classes, in many instances we observed phenotypes with characteristics shared between two or more groups. For example, several mutations affect the size of the wing, the patterning of veins, and the formation of the wing margin (Figures 4, D–F, and 5E). In these cases, we crossed representative alleles with members of several phenotypic classes to establish the complementation groups. The phenotypes of mosaic wings for all new alleles identified and for a representative allele of all known complementation groups isolated in the screen in combination with the Gal4 lines *sal^{EPv}-Gal4* and *638-Gal4* are shown in supporting information, Figure S1, Figure S2, Figure S3, and Figure S4.

Cytological mapping of novel mutants: To determine the cytological position of the new complementation groups, we used a collection of 36 chromosomal deficiencies that together cover the majority of the 2L arm (Figure 6A) and crossed them with 1 mutant (16 alleles) representing each complementation group and with 53 single mutants from the 55 single mutants identified in the screening. To identify gaps in the coverage of the 2L arm by these deficiencies, we also determined the viability of *trans*-heterozygous combinations between pairs of adjacent deletions, assuming that combinations between overlapping deficiencies are lethal. Using this criterion, we found that from the possible 35 pairwise combinations between adjacent deficiencies only 13 were lethal (Figure S5), suggesting that at least 22 small chromosomal intervals are not covered by these 36 deficiencies (Figure 6A). Using mainly lethality to define noncomplementation, we mapped to particular cytological intervals 12 of the 16 complementation groups formed by more than one allele (Figure 6B and Table 1). For individual mutations (55) we found 8 that complemented all deficiencies, 30 that failed to complement only one deficiency (Figure 6B and Table 1), and 17 that failed to complement two or more deficiencies (Figure 6C and Table 1). As we know which deficiencies overlap, those mutations that do not complement two adjacent deficiencies (2) were placed in the cytological region of overlap.

The complementation group formed by *77A2* and *133A1* corresponds to *med15*: We chose the complementation group formed by the alleles *77A2* and *133A1* to carry out an in-depth analysis of the affected gene. These alleles cause in mosaic wings a strong reduction of wing size, accompanied by the loss of the L2 vein and the differentiation of some ectopic bristles along the

A

Name	Cytology	Nº alleles	Nº AA
cdc2	31D11	1	297
ex	21C2	1	1427
ed/fred	24D4-6	1	1332
net	21B1	2	360
mad	23D3	2	455
PKA	30C1	2	353
S	21E4	2	597
Su(H)	35B8	4	594
smo	21B7	4	1036
fat	24D8	6	5147
kuz	34C4-6	6	1200
tkv	25D1	8	563

B

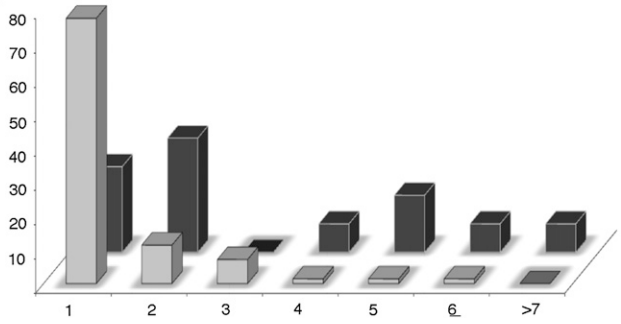

Figure 3.—General results of the screen. (A) Known genes identified in the screen, indicating their names ("Name"), cytological position ("Cytology"), number of alleles found ("No. alleles"), and the number of amino acids of the corresponding proteins ("No. AA"). (B) Relationship between the numbers of complementation groups (vertical values) and the number of alleles included in each complementation group (horizontal values). Data with light shading correspond to the new complementation groups identified in this screen and data with solid shading to genes that were known to play a role in wing development.

veins L2 and L3 (Figure 7). Both *77A2* and *133A* fail to complement *Df(2L)al* (21B8–C1;21C8–D1), and within the interval covered by this deficiency, *77A2* and *133A1* failed to complement *Df(2L)BSC107*, which deletes the 21C5;21D1 region (Figure 7A). There are 20 annotated genes in this interval, and we generated a smaller deficiency by FRT-mediated recombination between the Piggybac insertions *XP(+)d00080* and *WH(-)f06555*. This deficiency includes only 8 genes and fails to complement the alleles *77A2* and *133A1* (Figure 7A). Finally, we combined *77A2* and *133A1* with mutations in the genes *cabut* (*cbt*) and *med15* and found that both *77A2* and *133A1* are lethal in combination with $med15^{f04180}$ and viable in combination with a *cbt* allele (Figure 7A). *Med15* encodes a 749-amino-acid protein characterized by the presence of a Kix domain, two small poly(Q) stretches, and several LXXLL motifs (Gelbart *et al.* 1997; Figure 7B). We were able to map the *133A1* allele to the *med15* coding region by sequencing genomic regions amplified by PCR from homozygous *133A1* embryos (see materials and methods). This mutation is associated with a C to T transition that introduces a stop codon in the region that corresponds to the N-terminal poly(Q) localized after the KIX domain (Figure 7C). Using the same approach we could not find any nucleotide change in the coding region of *med15* in the *77A2* allele. Mitotic recombination clones of the $med15^{f04180}$ allele, generated in *638-Gal4*; $med15^{f04180}$ *FRT40A; M(2)z FRT40A; UAS-FLP/+* flies, result in smaller than wild-type wings with a normal pattern of veins (Figure 7H), suggesting that this allele is weaker than the novel *77A2* (Figure 7G) and *133A1* (Figure 7F) mutations. Homozygous *133A1* die during embryogenesis, and although some homozygous *77A2* embryos can hatch, they die during the first larval instar (data not shown). We have not studied the embryonic phenotypes of *med15* homozygous alleles.

The most characteristic phenotypes of *med15* alleles in the wing are loss of the L2 vein and a reduction in the size of the wing (Figure 7, F–H). These phenotypes were observed in mosaic wings generated in *638-Gal4; med15 FRT40A/M(2)z FRT40A; UAS-FLP/+* flies. We generated mitotic recombination clones of *med15* alleles in *hsFLP* f^{36a}*; med15 al dp b pr FRT40A/M(2)z* $[f^{+}]$ *FRT40A* males, because in this case the clones are labeled with the cell marker *forked* (*f*), and this allows the study of the autonomy of the clonal phenotypes. We could generate large *med15* M^{+} mutant clones when they were induced 48–72 h AEL, and in all cases the *med15* alleles behave in a cell autonomous manner. Thus, when the clones occupy the region between the L3 and L4 veins ($n = 4$), the size of this territory is strongly reduced (compare Figure 7I and 7J), and when the clones include the ventral L2 vein ($n = 10$) or the dorsal L4 vein ($n = 5$), these veins are reduced or absent (Figure 7, K and L). *Med15* clones running along the dorsal L3 vein diminish the pigmentation of the vein, but do not eliminate its differentiation ($n = 4$, data not shown). Similarly, clones affecting the proximal regions of L3, L4, and L5 do not affect vein differentiation (data not shown). We also studied the phenotypes resulting from the expression in the wing disc of interference RNA directed against *med15* (*med15-i*). In these flies, we observe a reduction in the size of the wing, the formation of some ectopic sensory organs, and only in some cases the loss of the L2 vein (Figure 7, N–P). Finally, we also found a requirement for *med15* in other tissues such as the thorax and legs. In the first case, the more frequent phenotype was a failure of the left and right hemithoraxes to fuse when one or both hemithoraxes are composed of *med15* mutant cells (Figure 7, Q and R). In the legs, we found many cases of legs with severe shortening along their entire length, accompanied by fusions of tarsal segments (not shown). These phenotypes are fully penetrant when the posterior compartments of the legs are composed of *med15* cells, as happens in *w;* $med15^{77A2}$ *al dp b pr FRT40A/M(2)z* $[f^{+}]$ *FRT40A; UAS-FLP/hh-Gal4* flies (Figure 7, T and T′, compare with Figure 7S). In general, the *med15* phenotypes are reminiscent of those caused by reduced *dpp* and TGFβ signaling, which consist of loss of veins, failures in dorsal closure, leg morphogenesis

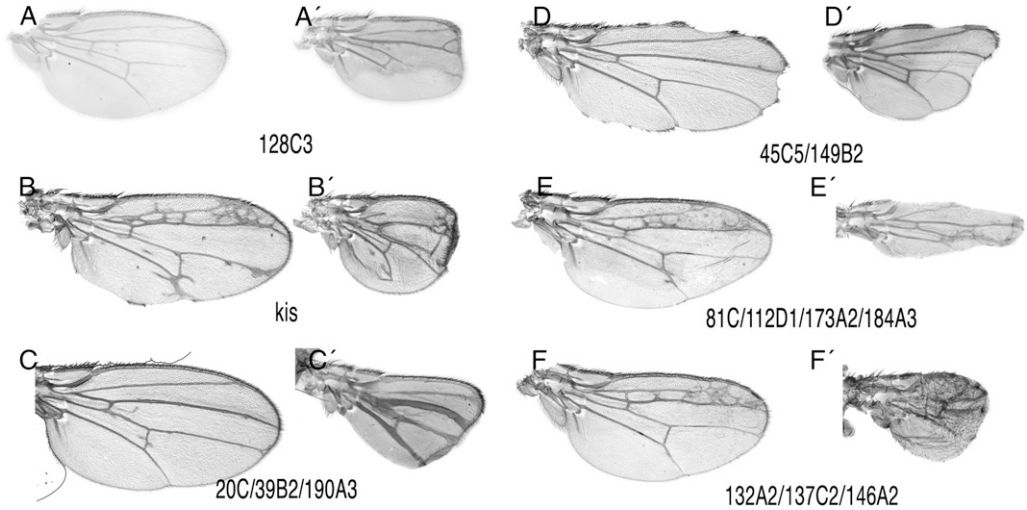

FIGURE 4.—Representative wings of the phenotypic classes affecting the formation of veins. (A and A′) Loss of veins and reduced wing size in *sal^{EPv}-Gal4; M(2)Z FRT40A/al dp b pr 128C3 FRT40A; UAS-FLP/+* (A) and *638-Gal4; M(2)Z FRT40A/al dp b pr 128C3 FRT40A; UAS-FLP/+* (A′). (B and B′) Loss and gain of veins in *sal^{EPv}-Gal4; M(2)Z FRT40A/al dp b pr 61C FRT40A; UAS-FLP/+* (B) and *638-Gal4; M(2)Z FRT40A/al dp b pr 61C FRT40A; UAS-FLP/+* (B′). The mutant *61C* is an allele of *kismet* (*kis*). (C and C′) Thick vein phenotype in *sal^{EPv}-Gal4; M(2)Z FRT40A/al dp b pr 20C FRT40A; UAS-FLP/+* (C) and *638-Gal4; M(2)Z FRT40A/al dp b pr 20C FRT40A; UAS-FLP/+* (C′). (D and D′) Wing margin phenotype of *sal^{EPv}-Gal4; M(2)Z FRT40A/al dp b pr 45C5 FRT40A; UAS-FLP/+* (D) and *638-Gal4; M(2)Z FRT40A/al dp b pr 45C5 FRT40A; UAS-FLP/+* (D′). (E and E′) Ectopic veins and loss of wing margin in *sal^{EPv}-Gal4; M(2)Z FRT40A/al dp b pr 81C FRT40A; UAS-FLP/+* (E) and *638-Gal4; M(2)Z FRT40A/al dp b pr 81C FRT40A; UAS-FLP/+* (E′). (F and F′) Ectopic veins and reduction in wing size in *sal^{EPv}-Gal4; M(2)Z FRT40A/al dp b pr 132A2 FRT40A; UAS-FLP/+* (F) and *638-Gal4; M(2)Z FRT40A/al dp b pr 132A2 FRT40A; UAS-FLP/+* (F′). The phenotypes of other mutations affecting the veins or the wing margin are shown in Figure S1 and Figure S3.

defects (Dpp), and reduced wing size (TGFβ) (POSAKONY *et al.* 1990; DE CELIS 1997; LECUIT and COHEN 1997; BRUMMEL *et al.* 1999; HARDEN 2002).

We also observed several alterations in gene expression patterns in *med15* mutant cells during imaginal development. For example, the expression of Bs is reduced in intervein territories formed by *med15* cells (Figure 8, A and B), suggesting that the transcriptional response to Dpp and Hedgehog signaling requires Med15 activity. Similarly, the expression of *spalt* (*sal*), a direct target of Dpp signaling (DE CELIS *et al.* 1996; BARRIO and DE CELIS 2004), is absent in *med15* clones localized in the anterior and posterior regions of the Sal domain of expression (Figure 8, C and D) and is reduced in clones localized in the central domain of *sal* expression (Figure 8, C and D). These effects are always cell autonomous, suggesting that Med15 does not affect *dpp* expression but compromises the capability of

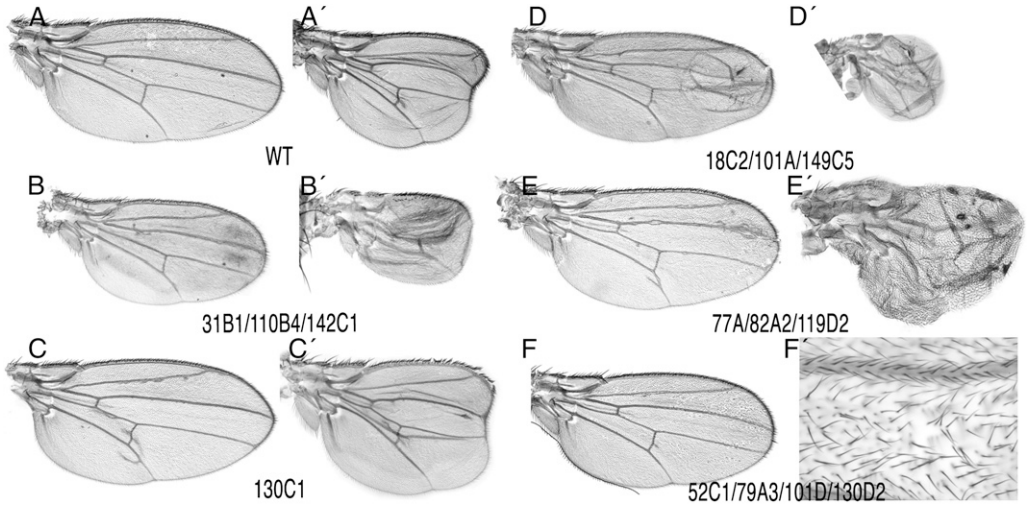

FIGURE 5.—Representative wings of the phenotypic classes affecting wing size, cell adhesion, and cell differentiation. (A and A′) Wild-type wing of *sal^{EPv}-Gal4; M(2)Z FRT40A/al dp b pr FRT40A; UAS-FLP/+* (A) and *638-Gal4; M(2)Z FRT40A/al dp b pr FRT40A; UAS-FLP/+* (A′) genotypes. (B and B′) Reduced wing size in *sal^{EPv}-Gal4; M(2)Z FRT40A/al dp b pr 31B1 FRT40A; UAS-FLP/+* (B) and *638-Gal4; M(2)Z FRT40A/al dp b pr 31B1 FRT40A; UAS-FLP/+* (B′). (C and C′) Increased wing size in *sal^{EPv}-Gal4; M(2)Z FRT40A/al dp b pr 130C1 FRT40A; UAS-FLP/+* (C) and *638-Gal4; M(2)Z FRT40A/al dp b pr 130C1 FRT40A; UAS-FLP/+* (C′). (D and D′) Failures in dorso-ventral adhesion in *sal^{EPv}-Gal4; M(2)Z FRT40A/al dp b pr 18C2 FRT40A; UAS-FLP/+* (D) and *638-Gal4; M(2)Z FRT40A/al dp b pr 18C2 FRT40A; UAS-FLP/+* (D′). (E and E′) Extra veins and increased wing size with loss of wing margin in *sal^{EPv}-Gal4; M(2)Z FRT40A/al dp b pr 77A FRT40A; UAS-FLP/+* (E) and *638G4-Gal4; M(2)Z FRT40A/al dp b pr 77A FRT40A; UAS-FLP/+* (E′). (F and F′) Formation of several trichomes per cell in *sal^{EPv}-Gal4; M(2)Z FRT40A/al dp b pr 52C1 FRT40A; UAS-FLP/+*. F′ is a higher magnification of the L3/L4 dorsal intervein. Other phenotypes affecting wing size, cell adhesion, and differentiation are shown in Figure S2 (size) and Figure S4 (adhesion and cell differentiation).

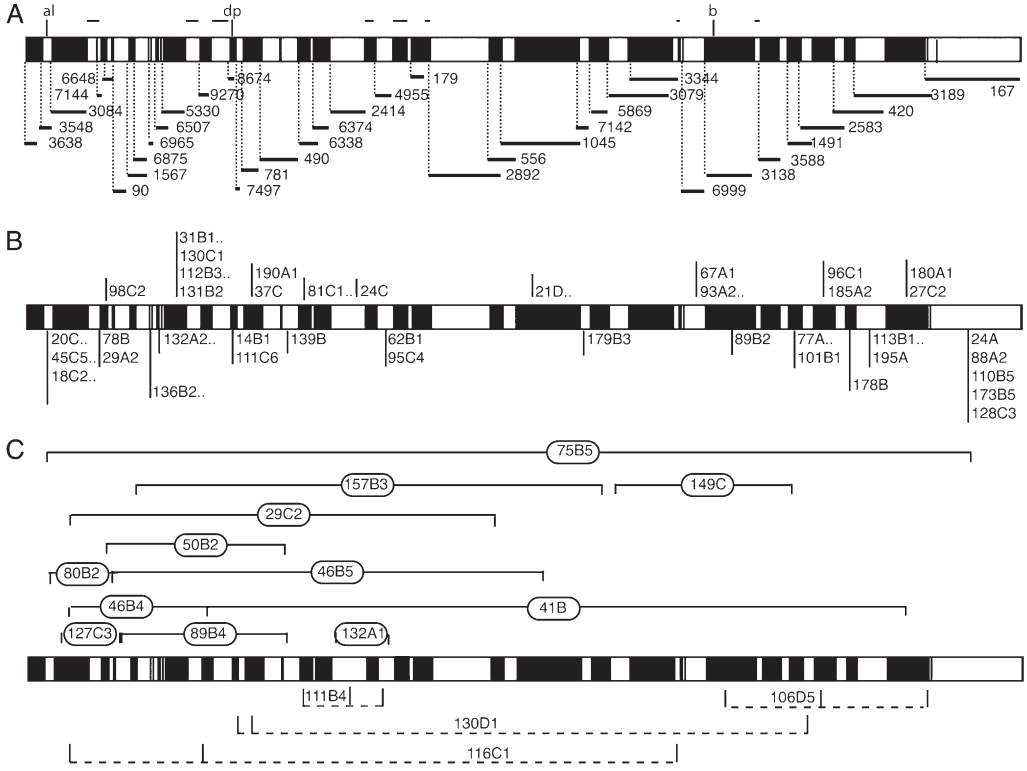

FIGURE 6.—Schematic representation of the complementation data with 2L deficiencies for all the mutants isolated. (A–C) The horizontal bars represent the chromosomal arm 2L subdivided in solid and open areas that exemplified the subdivision of the arm by the overlapping of the deficiencies used for the mapping. (A) Extent of the different deletions used for the complementation tests (see MATERIAL AND METHODS). The thin lines represent the main gaps left by the deficiencies. (B) Localization of mutants (single numbers) and complementation groups (single numbers and dots) that fail to complement with only one deficiency. (C) Localization of mutants that fail to complement with more than one deficiency.

Dpp signaling to activate its targets. A reduced response to Dpp signaling might also contribute to the smaller than normal wing size of *med15* mosaic wings and to the partial loss of vein stretches. We could not find changes in the expression of EGFR or Wingless target genes (*argos*, *Delta*, and *distalless*; data not shown), indicating that Med15 is not required as a general coactivator of transcription, but rather that its function is specific to particular enhancer–promoter interactions.

Other members of the Med complex are required during wing development: The involvement of *med15* in wing disc development suggests that other members belonging to the Med complex would be required in similar processes. Alternatively, *med15* functions might be independent of its participation in the Med complex. We studied the loss-of-function phenotypes of several Med complex components by driving the expression of specific interference RNAs in the wing disc. In all cases analyzed, we found that the reduction in Med expression gave rise to smaller than normal wings (*med10-i*, *med16-i*, *med25-i*, *med27-I*, and *kto-i*; Figure 9), which were extreme in the cases of loss of *med20* and *med30* (Figure 9). Only the reduction in *med20* and *med30* expression resulted in loss of vein phenotypes (Figure 9). In the cases of *med20*, *med30*, and *med15*, the expressions of their interference RNAs induce cell death (see Figure 8, E–H). In summary, and although the phenotypes observed upon a reduction in the expression of various Med components are not identical, they are similar enough to suggest that they could be caused by different degrees of loss of Mediator function.

DISCUSSION

The patterning of the veins and the growth of the wing involve the activities of several conserved signaling pathways and transcription factors, and mutations in these genes result in modifications of vein positioning and wing size (SOTILLOS and DE CELIS 2005). We have carried out a mosaic screen to search for mutations in the 2L chromosomal arm that modify the pattern of veins and the growth of the wing. In this screen we generated homozygous wing regions in otherwise heterozygous flies using a combination of the FRT-FLP method and the Gal4-UAS system. We maximize the fraction of the wing occupied by homozygous mutant cells using a *Minute* mutation. This also allows the survival of mutants cells that otherwise could be outcompeted by the surrounding wild-type cells (MORATA and RIPOLL 1975). The inconvenience of using a *Minute* mutation is that stocks and crosses involving this allele are less healthy. In general, the flies heterozygous for newly induced mutations with mosaic wings were viable and fertile, allowing the screening of a high number of treated chromosomes.

We identified 140 mutations and grouped them in 83 complementation groups, of which 12 correspond to previously known genes and 71 to alleles in other not yet identified genes. Among the genes previously known for their roles in wing formation we found 39 alleles affecting *net*, *mad*, *PKA*, *S*, *su(H)*, *smo*, *kuz*, *ex*, *ed/fred*, *cdc2*, *ft*, and *tkv*. The number of alleles in each complementation group was much higher in the case of the

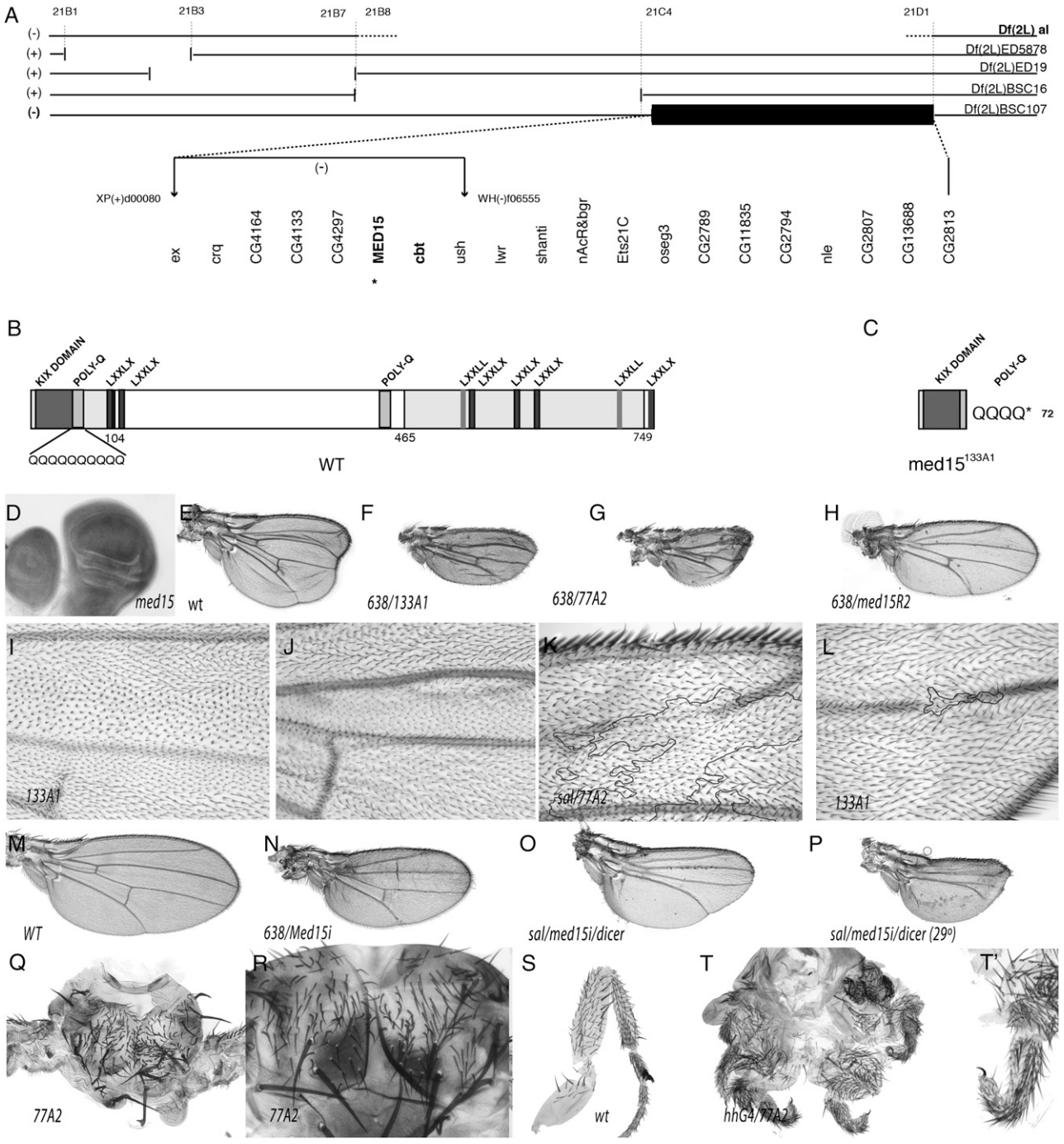

Figure 7.—The complementation group formed by *77A2* and *133A1* corresponds to *med15*. (A) Chromosomal interval 21B3–21C4 and extent of the deficiencies used (named to the right) shown as open spaces between horizontal bars. The region included in Df(2L)BSC107, which defines the localization of the 77A2/133A1 complementation group, is shown as a solid bar, and the genes included in this deficiency are shown at the bottom. The position of two PiggyBac insertions used to generate the *Df(2L)d0080-f06555* chromosome is shown by vertical arrows. (B) Protein sequence and domains of Med15. (C) Expected protein produced by the $med15^{133A1}$ allele. (D) Generalized expression of *med15* in the wing disc. (E) Control wing of *638-Gal4/+; FRT40A al dp b pr/FRT40A M(2)z; UAS-FLP/+* genotype showing the characteristic *dp* phenotype. (F and G) Homozygous wings for the *med15* alleles $med15^{133A1}$ (133A1) (E) and $med15^{77A2}$ (77A2) (F). The genotypes of these wings are *638-Gal4/+; FRT40A al* $med15^{133A1}$ *dp b pr/FRT40A M(2)z; UAS-FLP/+* (F) and *638-Gal4/+; FRT40A al* $med15^{77A2}$ *dp b pr/FRT40A M(2)z; UAS-FLP/+* (G). (H) Phenotype of $med15^{f04180}$ homozygous wing in *638-Gal4/+; FRT40A al* $med15^{f04180}$ *dp b pr/FRT40A M(2)z; UAS-FLP/+* female flies (compare the wing size with its control shown in M). (I and J) Mitotic recombination clones generated in *hsFLP1.22* f^{36a}*; ck P[f+]30C FRT40A/al* $med15^{133A1}$ *dp b pr FRT40A* flies. The clone in I is labeled with *ck* and is wild type for the *med15* gene (twin spot). The clone in J is labeled with *forked* and is homozygous for the $med15^{133A1}$ allele. Both clones are located in the L3/L4 intervein, occupying a large fraction of this dorsal (I) and ventral (J) intervein. (K) $med15^{77A2}$ clone labeled with *forked* generated in f^{36a} sal^{EPv}*-Gal4/+; FRT40A al* $med15^{77A2}$ *dp b pr/FRT40A P[f+]30C M(2)z; UAS-FLP/+* flies. The *forked* territory is enclosed by a solid line and is

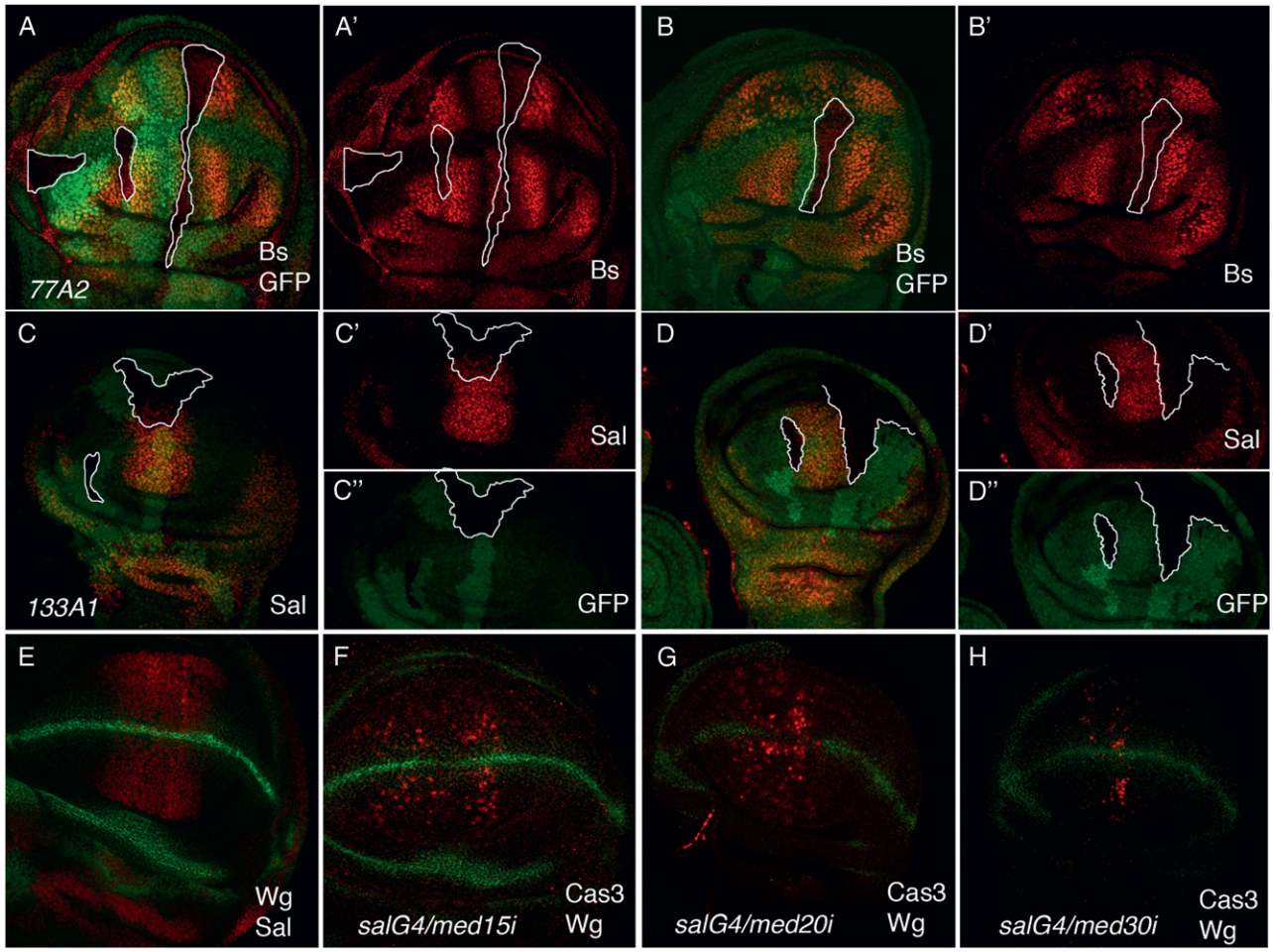

FIGURE 8.—Developmental analysis of *med15* function in the wing disc. (A and B) Expression of Bs (red) in $med15^{77A2}$ clones induced in flies of genotype *hsFLP1.22; P[tubGFP] FRT40A/*$med15^{77A2}$ *FRT40A* (twin clones). $med15^{77A2}$ clones are labeled by the absence of GFP (green) and each clone is encircled in a white line in A–B'. A′ and B′ are the corresponding red channels showing reduced Bs expression in the mutant clones. (C and D) Expression of Sal (red) in $med15^{133A1}$ clones induced in flies of genotype *hsFLP1.22; P[tubGFP] FRT40A/*$med15^{133A1}$ *FRT40A* (twin clones). $med15^{133A1}$ clones are labeled by the absence of GFP (green) and each clone is encircled in a white line in C and D, C′ and D′, and C″ and D″. ′ and ″ are the corresponding red (Sal) and green (GFP) channels, respectively. The expression of Sal is reduced or absent in mutant clones located in the center (C′) or lateral (D′) regions of the Sal domain, respectively. (E) Expression of Wingless (Wg, green) and Sal (Sal, red) in a wild-type third instar wing blade. (F–H) Induction of cell death (shown as expression of activated Caspase 3) (red in F–H) in flies expressing interference RNA in the *spalt* domain in sal^{EPv}*-Gal4/UAS-med15-RNAi* (F), sal^{EPv}*-Gal4/UAS-med20-RNAi* (G), and sal^{EPv}*-Gal4/UAS-med30-RNAi* (H).

known genes, as only 16 of 71 novel complementation groups were formed by more than one allele. These numbers indicate that the screen is not yet at saturation and that the visibility of the phenotypes is much higher in wings homozygous for mutations in the class of known genes. We were able to map 58% of the complementation groups to individual chromosomal intervals using a collection of deficiencies that cover an estimated 80% of the 2L arm. However, these data have several caveats due to the high number of complementation groups formed by only one allele and to the presence in the treated chromosomes of associated lethals. Thus, 23% of the novel complementation groups failed to complement with more than one deficiency, and

associated with the loss of the ventral L2 vein. (L) Small $med15^{133A1}$ clone in the distal dorsal L4 vein causing the loss of this vein. (M–P) Phenotypes resulting from the expression of *med15* interference RNA (*med15i*) in the genotypes *638-Gal4/+; UAS-med15i* (N), sal^{EPv}*-Gal4/UAS-med15i; UAS-dicer/+* (O), and sal^{EPv}*-Gal4/UAS-med15i; UAS-dicer/+* grown at 29° (P). The wild-type control wing is shown in M. (Q and R) Two examples of thoraxes taken at different magnification showing the failure in the fusion between the left and the right hemithorax when the central region is occupied by $med15^{77A}$ mutant cells (labeled with *forked* in *hsFLP1.22* f^{36a}*; P[f+]30C M(2)z FRT40A/al* $med15^{77A2}$ *dp b pr FRT40A* flies). (S) Wild-type male first leg. (T and T′) Two examples of legs taken at different magnifications (T′ is ×4 T) showing the defects in leg morphogenesis and tarsal segmentation in *w; M(2)z P[f+]30C FRT40A/al* $med15^{77A}$ *dp b pr FRT40A; hh-Gal4/UAS-FLP* flies.

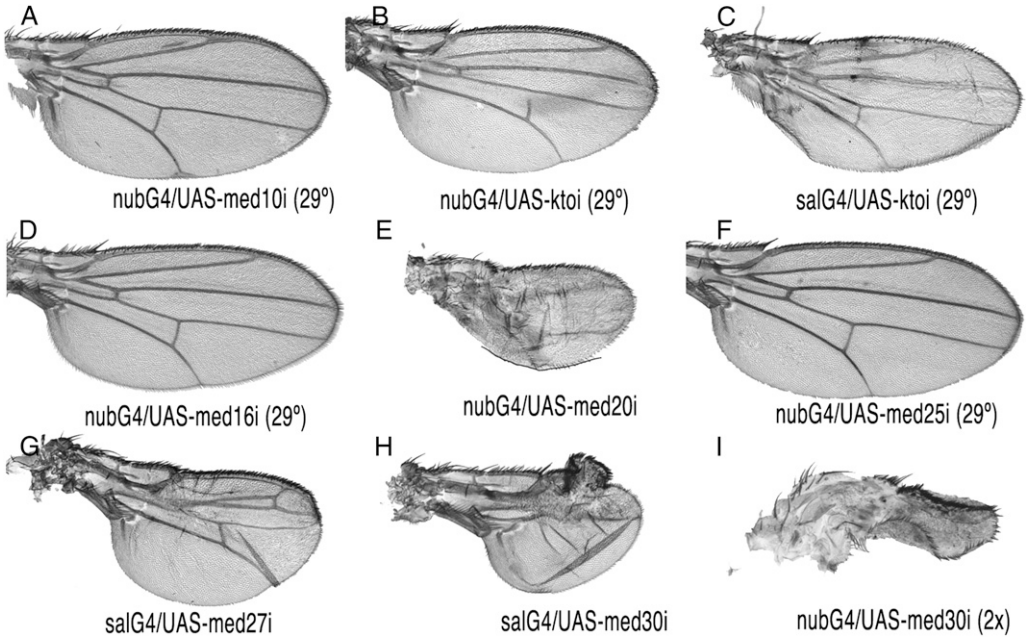

Figure 9.—Wing phenotypes caused by reduced expression of different components of the Mediator complex. (A–I) Adult wings of Gal4/UAS-RNAi combinations showing smaller than normal size and different defects in the patterning of veins. (A) *nub-Gal4/UAS-med10i* at 29°. (B) *nub-Gal4/UAS-ktoi* (29°). (C) *sal^{EPv}-Gal4/UAS-ktoi* (29°). (D) *nub-Gal4/UAS-med16i* (29°). (E) *nub-Gal4/UAS-med20i.* (F) *nub-Gal4/UAS-med25i* (29°). (G) *sal^{EPv}-Gal4/UAS-med27i.* (H) *sal^{EPv}-Gal4/UAS-med30i.* (I) *nub-Gal4/UAS-med30i* (taken at magnification ×2).

11% of complementation groups complemented for lethality and phenotype with all deficiencies. In this manner, the cytological localization of all complementation groups composed by only one allele is still tentative. The phenotypes identified in the screen mainly affected the wing veins and wing margin, the size of the wing, the adhesion between the dorsal and ventral wing surfaces, the integrity of the epithelium, and the differentiation of trichomes by wing cells. These phenotypes correspond to alterations in processes that occur during the third larval instar (vein determination, wing disc growth, and wing margin formation) and during pupal development (dorso-ventral adhesion and trichome differentiation). Furthermore, the observed phenotypes are informative about the process, and in some cases the pathways, that might be altered in the mutants. For example, changes in wing size without effects in vein formation are expected by modifications in the insulin and TGFβ pathways (Brummel *et al.* 1999; Johnston and Gallant 2002), alterations in the integrity of the wing margin are a mark of loss of Notch and Wingless signaling at the dorso-ventral boundary (Couso *et al.* 1994; de Celis and Garcia-Bellido 1994), changes in the formation of veins are expected by modifications in the Dpp, EGFR, and Notch pathways (Sotillos and de Celis 2005), and the formation of blistered wings is typical of defects in Integrin and Laminin functions (Walsh and Brown 1998; Urbano *et al.* 2009). Future work will aim to unambiguously map the different complementation groups to individual genes and to identify the developmental functions they affect.

We chose to analyze in some detail the complementation group formed by the *77A* and *133A1* mutants. These mutations are alleles of *med15*, a gene encoding one component of the Mediator complex (Guglielmi *et al.* 2004). Thus, they fail to complement other *med15* alleles, and *med15^{133A1}* is associated with a stop codon that could truncate the protein in the N-terminal region after the KIX domain. The Mediator multiprotein complex promotes the transcription of inducible genes, acting as a link between the RNApolII holoenzyme and several sequence-specific transcription factors (Naar *et al.* 2001; Lewis and Reinberg 2003; Taatjes *et al.* 2004). The human homolog of Med15, MED105, is included in all Mediator complexes identified so far and forms part of a module named the tail that is the main target for the transcriptional activators (Guglielmi *et al.* 2004; Taatjes *et al.* 2004). Thus, Med15 homologs can bid to different transcription factors such as Gcn4 and Gal4 in *Saccharomyces cerevisiae* (Fishburn *et al.* 2005; Reeves and Hahn 2005), SREBP in *Caenorhabditis elegans* (Taubert *et al.* 2006; Yang *et al.* 2006), and, more interesting from the perspective of our data, to Smad2/3 and Smad4 in Xenopus (Kato *et al.* 2002). Other members of the Mediator complex that were previously analyzed are *kohtalo* and *skuld* (Med12 and Med13, respectively), which form part of the conserved Cdk8 module (Bourbon *et al.* 2004; Conaway *et al.* 2005; Kim and Lis 2005). Interestingly, mouse Cdk8 and Cdk9 phosphorylate Smad proteins, regulating their transcriptional activity and turnover (Alarcón *et al.* 2009). However, *kohtalo* and *skuld* are required for sensory organ development, for some aspects of Notch and Hedgehog signaling, and for the transcription of Wingless downstream genes (Janody *et al.* 2003; Carrera *et al.* 2008).

Med15 mutations result in smaller than normal wings and loss of mainly the L2 vein. They also affect the fusion between the left and the right hemithorax and leg morphogenesis. The reduction in the level of

expression of other components of the Mediator complex, most notably *med20*, *med27*, and *med30*, also results in smaller than normal wings and failures in vein differentiation, in addition to causing some levels of cell death. Although these phenotypes were similar, they are not identical, which might indicate specific requirements of these subunits or, alternatively, a different degree in the effectiveness of each interference RNA used. Mutant *med15* cells display specific defects in gene expression, suggesting a requirement limited to particular enhancer–promotor interactions. In particular, the expression of *spalt*, a direct target of Dpp signaling, is compromised in *med15* mutant cells. There are no known transcriptional targets of TGFβ signaling in the wing, and consequently we could not determine directly whether the activity of this pathway is diminished in *med15* mutants. A direct requirement of Med15 for the transcription of TGFβ target genes is nonetheless suggested by the similar phenotypes of wing size reduction observed in *med15* mutants and in *baboon* mutations (Brummel *et al.* 1999).

We are very grateful to Rosario Hernández and Cristina Prieto for their technical assistance. This work was supported by grants BFU2006-06501 and Consolider CSD-2007-00008 from the Spanish Ministry of Research and Innovation. An institutional grant from the Ramón Areces Foundation to the Centro de Biología Molecular "Severo Ochoa" is also acknowledged.

LITERATURE CITED

Alarcón, C., A.-I. Zaromytidou, Q. Xi, S. Gao, J. Yu *et al.*, 2009 Nuclear CDKs drive Smad transcriptional activation and turnover in BMP and TGF-b pathways. Cell **139:** 757–769.

Ashburner, M., 1989 *Drosophila. A Laboratory Manual.* Cold Spring Harbor Laboratory Press, Cold Spring Harbor, NY.

Baker, N. E., 1987 Molecular cloning of sequences from wingless a segment polarity gene in Drosophila the spatial distribution of a transcript in embryos. EMBO J. **6:** 1765–1774.

Barrio, R., and J. F. de Celis, 2004 Regulation of *spalt* expression in the *Drosophila* wing blade in response to the Decapentaplegic signaling pathway. Proc. Natl. Acad. Sci. USA **101:** 6021–6026.

Bier, E., 2000 Drawing lines in the *Drosophila* wing: initiation of wing vein development. Curr. Opin. Genet. Dev. **10:** 393–398.

Boedigheimer, M., P. Bryant and A. Laughon, 1993 Expanded, a negative regulator of cell proliferation in *Drosophila*, shows homology to the NF2 tumor suppressor. Mech. Dev. **44:** 83–84.

Bourbon, H. M., A. Aguilera, A. Z. Ansari, F. J. Asturias, A. J. Berk *et al.*, 2004 A unified nomenclature for protein subunits of mediator complexes linking transcriptional regulators to RNA polymerase II. Mol. Cell **14:** 553–557.

Brentrup, D., H. P. Lerch, H. Jackle and M. Noll, 2000 Regulation of *Drosophila* wing vein patterning: *net* encodes a bHLH protein repressing *rhomboid* and is repressed by rhomboid dependent EGFR signalling. Development **127:** 4729–4741.

Brummel, T., S. Abdollah, T. E. Haerry, M. J. Shimell, J. Merriam *et al.*, 1999 The *Drosophila* Activin receptor Baboon signals through dSmad2 and controls cell proliferation but not patterning during larval development. Genes Dev. **13:** 98–111.

Calleja, M., E. Moreno, S. Pelaz and G. Morata, 1996 Visualization of gene expression in living adult *Drosophila*. Science **274:** 252–255.

Carrera, I., F. Janody, N. Leeds, F. Duveau and J. E. Treisman, 2008 Pygopus activates Wingless target gene transcription through the mediator complex subunits Med12 and Med13. Proc. Natl. Acad. Sci. USA **105:** 6644–6649.

Chen, Y., and G. Struhl, 1996 Dual roles for Patched in sequestering and transducing Hedgehog. Cell **87:** 553–563.

Clegg, N. J., I. P. Whitehead, J. A. Williams, G. B. Spiegelman and T. A. Grigliatti, 1993 A developmental and molecular analysis of *Cdc2* mutations in Drosophila melanogaster. Genome **36:** 676–685.

Cohen, S. M., 1993 *Imaginal Disc Development.* Cold Spring Harbor Laboratory Press, Cold Spring Harbor, NY.

Conaway, R. C., S. Sato, C. Tomomorisato, T. Yao and J. W. Conaway, 2005 The mammalian Mediator complex and its role in transcriptional regulation. Trends Biochem. Sci. **30:** 250–255.

Couso, J. P., S. A. Bishop and A. Martinez Arias, 1994 The wingless signalling pathway and the patterning of the wing margin in *Drosophila.* Development **120:** 621–636.

Cruz, C., A. Glavic, M. Casado and J. F. de Celis, 2009 A gain of function screen identifying genes required for growth and pattern formation of the *Drosophila melanogaster* wing. Genetics **183:** 122.

de Celis, J. F., 1997 Expression and function of *decapentaplegic* and *thick veins* in the differentiation of the veins in the *Drosophila* wing. Development **124:** 1007–1018.

de Celis, J. F., 2003 Pattern formation in the *Drosophila* wing: the development of the veins. BioEssays **25:** 443–451.

de Celis, J. F., and A. Garcia-Bellido, 1994 Roles of the *Notch* gene in *Drosophila* wing morphogenesis. Mech. Dev. **46:** 109–122.

de Celis, J. F., R. Barrio and F. C. Kafatos, 1996 A gene complex acting downstream of Dpp in *Drosophila* wing morphogenesis. Nature **381:** 421–424.

Duffy, J. B., D. A. Harrison and N. Perrimon, 1998 Identifying loci required for follicular patterning using directed mosaics. Development **125:** 2263–2271.

Fishburn, J., N. Mohibullah, and S. Hahn, 2005 Function of a eukaryotic transcription activator during the transcription cycle. Mol. Cell **18:** 369–378.

Freeman, M., 1994 The *spitz* gene is required for photoreceptor determination in the *Drosophila* eye where it interacts with the EGF receptor. Mech. Dev. **48:** 25–33.

Fristrom, D., P. Gotwals, S. Eaton, T. Kornberg, M. A. Sturtevant *et al.*, 1994 *blistered*; a gene required for vein/intervein formation in wings of *Drosophila.* Development **120:** 2661–2686.

Garcia-Bellido, A., and J. Dapena, 1974 Induction, detection and characterization of cell differentiation mutants in *Drosophila.* Mol. Gen. Genet. **128:** 117–130.

Gelbart, W. M., M. Crosby, B. Matthews, W. P. Rindone, J. Chillemi *et al.*, 1997 FlyBase: a *Drosophila* database. The FlyBase consortium. Nucleic Acids Res. **25:** 63–66.

Guglielmi, B., N. L. V. Berkum, B. Klapholz, T. Bijma, M. Boube *et al.*, 2004 A high resolution protein interaction map of the yeast Mediator complex. Nucleic Acids Res. **32:** 5379–5391.

Hao, I., R. B. Green, O. Dunaevsky, J. A. Lengyel and C. Rauskolb, 2003 The oddskipped family of zinc finger genes promotes *Drosophila* leg segmentation. Dev. Biol. **263:** 282–295.

Harden, N., 2002 Signaling pathways directing the movement and fusion of epithelial sheets: lessons from dorsal closure in Drosophila. Differentiation **70:** 181–203.

Ito, K., W. Awano, K. Suzuki, Y. Hiromi and D. Yamamoto, 1997 The *Drosophila* mushroom body is a quadruple structure of clonal units each of which contains a virtually identical set of neurones and glial cells. Development **124:** 761–771.

Janody, F., Z. Martirosyan, A. Benlali and J. E. Treisman, 2003 Two subunits of the *Drosophila* mediator complex act together to control cell affinity. Development **130:** 3691–3701.

Johnston, L. A., and P. Gallant, 2002 Control of growth and organ size in Drosophila. BioEssays **24:** 54–64.

Kato, Y., R. Habas, Y. Katsuyama, A. M. Naar and X. He, 2002 A component of the ARC/Mediator complex required for TGF beta/Nodal signalling. Nature **418:** 641–646.

Kim, J., A. Sebring, J. J. Esch, M. E. Kraus, K. Vorwerk *et al.*, 1996 Integration of positional signals and regulation of wing formation by *Drosophila* vestigial gene. Nature **382:** 133–138.

Kim, Y. J., and J. T. Lis, 2005 Interactions between subunits of *Drosophila* Mediator and activator proteins. Trends Biochem. Sci. **30:** 245–249.

Kuang, B., S. C. Wu, Y. Shin, L. Luo and P. Kolodziej, 2000 *split ends* encodes large nuclear proteins that regulate neuronal cell

fate and axon extension in the *Drosophila* embryo. Development **127:** 1517–1529.

Kwon, J. Y., J. M. Park, B. S. Gim, S. J. Han, J. Lee *et al.*, 1999 *Caenorhabditis elegans* mediator complexes are required for developmental specific transcriptional activation. Proc. Natl. Acad. Sci. USA **96:** 14990–14995.

Lecuit, T., and S. M. Cohen, 1997 Proximal distal axis formation in the *Drosophila* leg. Nature **388:** 139–145.

Lewis, B. A., and D. Reinberg, 2003 The mediator coactivator complex: functional and physical roles in transcriptional regulation. J. Cell Sci. **116:** 3667–3675.

Li, W., J. Talavera, M. Lane and D. Kalderon, 1995 Function of protein kinase A in hedgehog signal transduction and *Drosophila* imaginal disc development. Cell **80:** 553–562.

Mahoney, P. A., U. Weber, P. Onofrechuk, H. Biessmann, P. J. Bryant *et al.*, 1991 The *fat* tumor suppressor gene in *Drosophila* encodes a novel member of the cadherin gene superfamily. Cell **67:** 853–868.

Montagne, J., J. Groppe, K. Guillemin, M. A. Krasnow, W. J. Gehring *et al.*, 1996 The Drosophila serum response factor gene is required for the formation of intervein tissue of the wing and is allelic to *blistered*. Development **122:** 2589–2597.

Morata, G., and P. Ripoll, 1975 *Minutes*: mutants of *Drosophila* autonomously affecting cell division rate. Dev. Biol. **42:** 211–221.

Morel, V., and F. Schweisguth, 2000 Repression by Suppressor of Hairless and activation by Notch are required to define a single row of singleminded expressing cells in the *Drosophila* embryo. Genes Dev. **14:** 377–388.

Naar, A. M., B. D. Lemon and R. Tjian, 2001 Transcriptional coactivator complexes. Annu. Rev. Biochem. **70:** 475–501.

Nellen, D., M. Affolter and K. Basler, 1994 Receptor serine/threonine kinases implicated in the control of Drosophila body pattern by decapentaplegic. Cell **78:** 225–237.

Parks, A. L., K. R. Cook, M. Belvin, N. A. Dompe, R. Fawcett *et al.*, 2004 Systematic generation of high resolution deletion coverage of the *Drosophila melanogaster* genome. Nat. Genet. **36:** 288–292.

Posakony, L. G., L. A. Raftery and W. M. Gelbart, 1990 Wing formation in *Drosophila melanogaster* requires *decapentaplegic* gene function along the anterior posterior compartment boundary. Mech. Dev. **33:** 69–82.

Prout, M., Z. Damania, J. Soong, D. Fristrom and J. W. Fristrom, 1997 Autosomal mutations affecting adhesion between wing surfaces in *Drosophila* melanogaster. Genetics **146:** 275–285.

Reeves, W. M., and S. Hahn, 2005 Targets of the Gal4 transcription activator in functional transcription complexes. Mol. Cell Biol. **25:** 9092–9102.

Ripoll, P., and A. Garcia-Bellido, 1979 Viability of homozygous deficiencies in somatic cells of *Drosophila melanogaster*. Genetics **91:** 443–453.

Roch, F., A. Baonza, E. Martin-Blanco and A. Garcia-Bellido, 1998 Genetic interactions and cell behaviour in *blistered* mutants during proliferation and differentiation of the *Drosophila* wing. Development **125:** 1823–1832.

Rogge, R., P. J. Green, J. Urano, S. Hornsaban, M. Mlodzik *et al.*, 1995 The role of *yan* in mediating the choice between cell division and differentiation. Development **121:** 3947–3958.

Rogge, R. D., C. A. Karlovich and U. Banerjee, 1991 Genetic dissection of a neurodevelopmental pathway: Son of sevenless functions downstream of the sevenless and EGF receptor tyrosine kinases. Cell **64:** 39–48.

Sotillos, S., and J. F. de Celis, 2005 Interactions between the Notch, EGFR, and decapentaplegic signaling pathways regulate vein differentiation during *Drosophila* pupal wing development. Dev. Dyn. **232:** 738–752.

Sotillos, S., F. Roch and S. Campuzano, 1997 The metalloprotease disintegrin Kuzbanian participates in Notch activation during growth and patterning of *Drosophila* imaginal discs. Development **124:** 4769–4779.

St. Johnston, R. D., F. M. Hoffmann, R. K. Blackman, D. Segal, R. Grimaila *et al.*, 1990 Molecular organization of the *decapentaplegic* gene in *Drosophila melanogaster*. Genes Dev. **4:** 1114–1127.

Taatjes, D. J., M. T. Marr and R. Tjian, 2004 Regulatory diversity among metazoan co-activator complexes. Nat. Rev. Mol. Cell Biol. **5:** 403–410.

Taubert, S., M. R. V. Gilst, M. Hansen and K. R. Yamamoto, 2006 A Mediator subunit, MDT15, integrates regulation of fatty acid metabolism by NHR49 dependent and independent pathways in *C. elegans*. Genes Dev. **20:** 1137–1149.

Urbano, J. M., C. Torgler, C. Molnar, A. López-Varea, N. Brown *et al.*, 2009 *Drosophila* laminins act as key regulators of basement membrane assembly and morphogenesis. Development **136:** 4165–4176.

Walsh, E. P., and N. H. Brown, 1998 A screen to identify *Drosophila* genes required for integrin mediated adhesion. Genetics **150:** 791–805.

Williams, J. A., J. B. Bell and S. B. Carroll, 1991 Control of *Drosophila* wing and haltere development by the nuclear vestigial gene product. Genes Dev. **5:** 2481–2495.

Xu, T., and S. D. Harrison, 1994 Mosaic analysis using FLP recombinase. Methods Cell Biol. **44:** 655–681.

Xu, T., W. Wang, S. Zhang, R. A. Stewart and W. Yu, 1995 Identifying tumor suppressors in genetic mosaics: the *Drosophila lats* gene encodes a putative protein kinase. Development **121:** 1053–1063.

Yang, F., B. W. Vought, J. S. Satterlee, A. K. Walker, Z. Y. Jim Sun *et al.*, 2006 An ARC/Mediator subunit required for SREBP control of cholesterol and lipid homeostasis. Nature **442:** 700–704.

Communicating editor: N. Perrimon

GENETICS

Supporting Information
http://www.genetics.org/cgi/content/full/genetics.109.113670/DC1

Identification of Genes Affecting Wing Patterning Through a Loss-of-Function Mutagenesis Screen and Characterization of *med15* Function During Wing Development

Ana Terriente-Félix, Ana López-Varea and Jose F. de Celis

DOI: 10.1534/genetics.109.113670

FIGURE S1.—Mosaic wings for mutations isolated in the screen in flies of *sal^{EPv}-Gal4/+; FRT40A mut al dp b pr/FRT40A M(2)z; UAS-FLP/+* (A-V) and *638-Gal4/+; FRT40A mut al dp b pr/FRT40A M(2)z; UAS-FLP/+* (A'-V'). In the cases of the mutations 128C3 and 88A2 it is shown the phenotype of mutant clones at higher (4x) magnification.

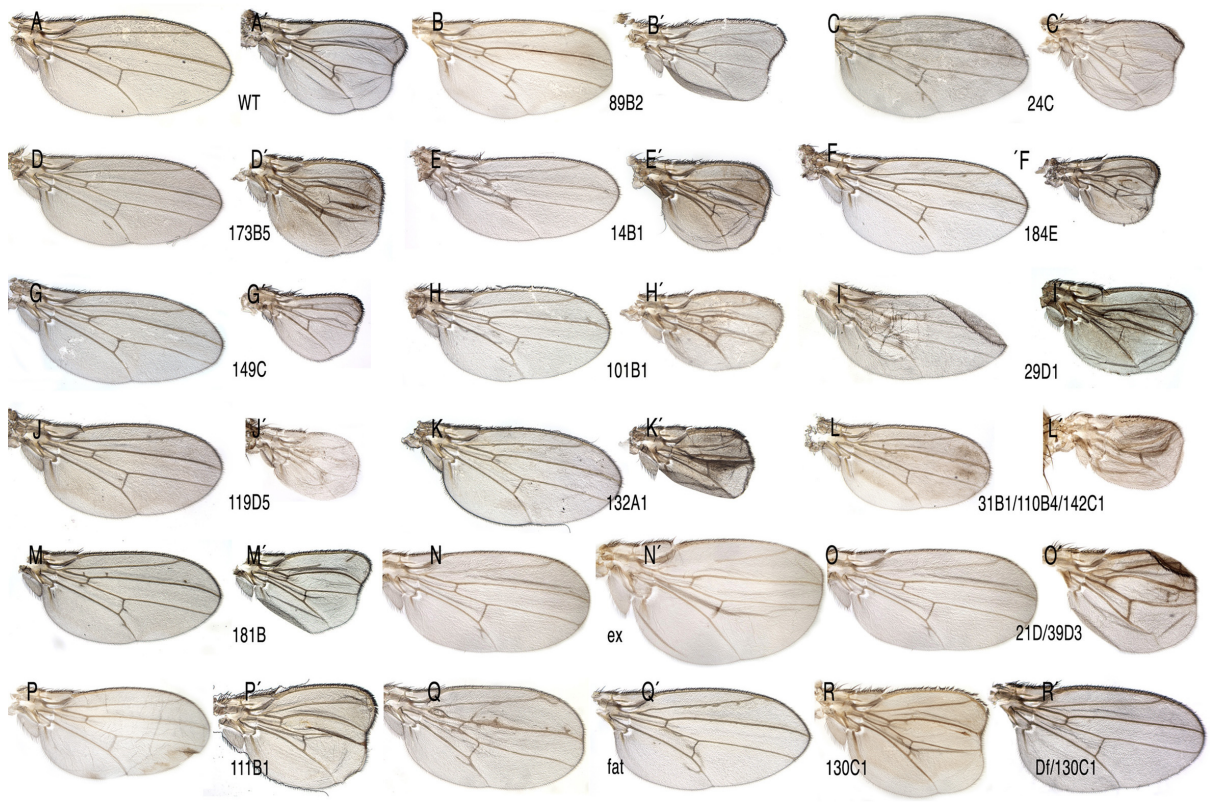

FIGURE S2.—Mosaic wings for mutations isolated in the screen in flies of *sal^{EPv}-Gal4/+; FRT40A mut al dp b pr/FRT40A M(2)z; UAS-FLP/+* (B-R) and *638-Gal4/+; FRT40A mut al dp b pr/FRT40A M(2)z; UAS-FLP/+* (B'-R'). A and A' correspond to control wings of *sal^{EPv}-Gal4/+; FRT40A al dp b pr/FRT40A M(2)z; UAS-FLP/+* (A) and *638-Gal4/+; FRT40A al dp b pr/FRT40A M(2)z; UAS-FLP/+* (A').

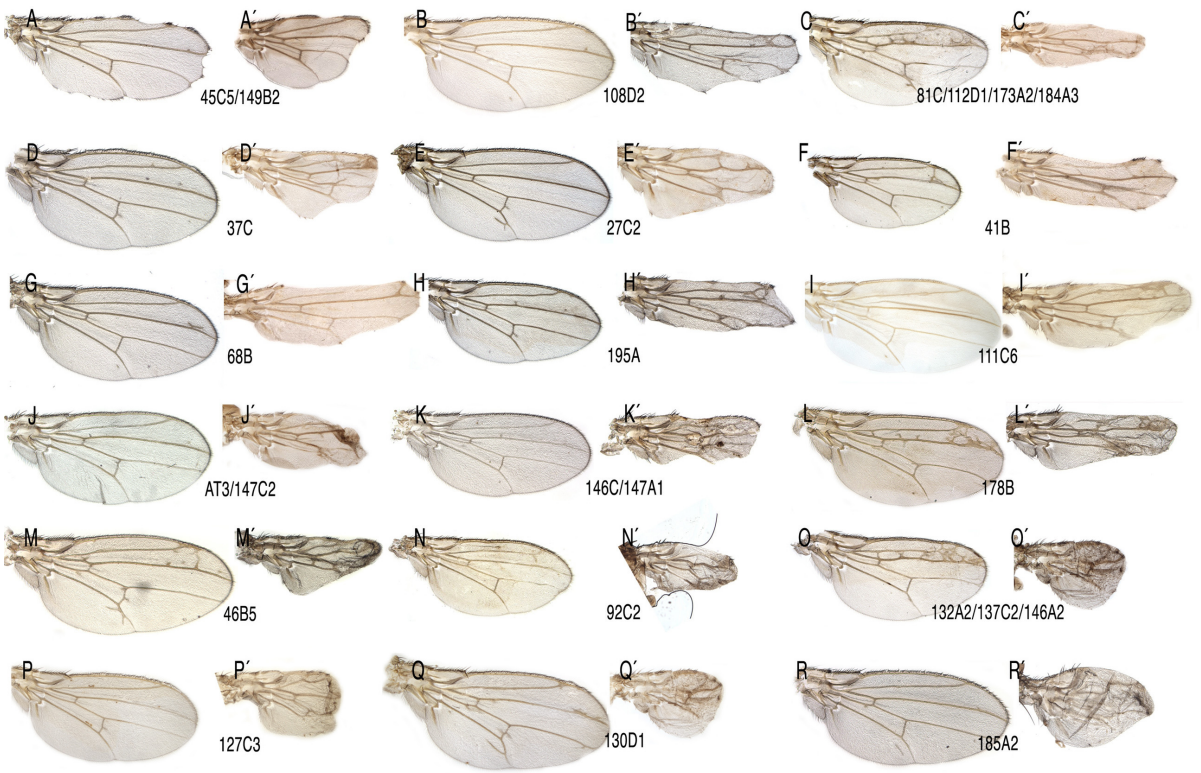

FIGURE S3.—Mosaic wings for mutations isolated in the screen in flies of *sal^{EPv}-Gal4/+; FRT40A mut al dp b pr/FRT40A M(2)z; UAS-FLP/+* (A-R) and *638-Gal4/+; FRT40A mut al dp b pr/FRT40A M(2)z; UAS-FLP/+* (A'-R').

FIGURE S4.—Mosaic wings for mutations isolated in the screen in flies of *sal^{EPv}-Gal4/+; FRT40A mut al dp b pr/FRT40A M(2)z; UAS-FLP/+* (A-P and R-V) and *638-Gal4/+; FRT40A mut al dp b pr/FRT40A M(2)z; UAS-FLP/+* (A'-P' and R''-V''). (R'-W' and R'''-U''') Pictures of the corresponding wings shown at higher magnification (4x) to show trichome differentiation in mosaic wings.

3638	Df(2L)net-PMF	21A1;21B7-8	VIABLE	
3548	Df(2L)al	21B8-C1;21C8-D1		LETHAL
3084	Df(2L)ast2	21D1-2;22B2-3	VIABLE	
7144	Df(2L)BSC37	22D2-3;22F1-2		VIABLE
6648	Df(2L)dpp[d14]	22E4-F2;22F3-23A1	VIABLE	
90	Df(2L)C144	22F4-23A1;23C2-4		VIABLE
1567	Df(2L)JS17	23C1-2;23E1-2	LETHAL	
6875	Df(2L)BSC28	23C5-D1;23E2		VIABLE
6965	Df(2L)BSC31	23E5;23F4-5	VIABLE	
6507	Df(2L)drm-P2	23F3-4;24A1-2		LETHAL
5330	Df(2L)ed1	24A2;24D4	VIABLE	
9270	Df(2L)ED250	24F4;25A7		VIABLE
8674	Df(2L)BSC109	25C4;25C8	VIABLE	
7497	Df(2L)Exel6011	25C8;25D5		VIABLE
781	Df(2L)cl-h3	25D2-4;26B2-5	VIABLE	
490	Df(2L)E110	25F3-26A1;26D3-11		VIABLE
6338	Df(2L)BSC6	26D3-E1;26F4-7	LETHAL	
6374	Df(2L)BSC7	26D10-E1;27C1		VIABLE
2414	Df(2L)spd[j2]	27C1-2;28A	VIABLE	
4955	Df(2L)XE-2750	028B02;028D03		VIABLE
179	Df(2L)TE29Aa-11	28E4-7;29B2-C1	VIABLE	
2892	Df(2L)N22-14	29C1-2;30C8-9		LETHAL
556	Df(2L)s1402	30C01-02;030F	LETHAL	
1045	Df(2L)Mdh	30D-30F;31F		LETHAL
7142	Df(2L)BSC32	32A1-2;32C5-D1	VIABLE	
5869	Df(2L)FCK-20	32D1;32F1-3		VIABLE
3079	Df(2L)Prl	32F1-3;33F1-2	LETHAL	
3344	Df(2L)prd1.7	33B2-3;34A1-2		VIABLE
6999	Df(2L)BSC30	34A3;34B7-9	LETHAL	
3138	Df(2L)b87e25	34B12-C1;35B10-C1		VIABLE
3588	Df(2L)TE35BC-24	35B4-6;35F1-7	VIABLE	
1491	Df(2L)r10	35E1-2;36A6-7		LETHAL
2583	Df(2L)cact-255rv64	35F-36A;36D	LETHAL	
420	Df(2L)TW137	36C2-4;37B9-C1		LETHAL
3189	Df(2L)TW50	036E04-F01;038A06-07	LETHAL	
167	Df(2L)TW161	38A6-B1;40A4-B1		

FIGURE S5.—Results of the combinations between the deficiencies used for the cytological mapping of the complementation groups. The deficiencies are named by its Bloomington Stock numbers (1st column) and by its original names (2nd column). Their breakpoints are indicated in the 3rd column. The 36 deficiencies were crossed in pairs between adjacent ones, and the results of these combinations are indicated in the right columns as VIABLE or LETHAL.

TABLE S1

Results of the mapping of complementation groups composed by two or more alleles

PHENOTYPE CLASS	MUTANTS	COMPLEMENTATION WITH DEFICIENCIES						RESULT
LOSS OF VEINS	**MED15**	3548						**3548**
ECTOPIC VEINS	**kismet**	3638						**3638**
	20C	1045	-	3548	5869			
THICKER VEINS	**39B2**	V	V	L	V			**3548**
	190A3	V	2892	-	V			
L3 DUPLICATION	**112B3**	3548	5330					**5330**
	147A2	V	L					
	31B1	7142	5330	V	167			
REDUCED SIZE	**110B4**	-	L	V	-			**5330**
	142C3	V	SL	V	V			
AUGMENTED SIZE	**21D**	1045	5869					**1045**
	39D3	L	V					
	52C1	1045	7142	2583				
CELL DIFFERENTATION	**79A3**	+V	L					**??**
	101D	V	V	-				
	130D2	V	V	-				
LOSS OF WING MARGIN	**45C5**	3548	3079	3344	6999			**3548**
	149B2	L	V	V	V			
	AT3	2583	6374					**??**
	147C2	V	V					
	81C	V	6338	179	V	6965		
	108D2	490	L		V	-	167	
	112D1	490	L		2892	V		**6338**
ECTOPIC VEINS + LOSS OF WING MARGIN	**173A2**	V	-		V	V		
	184A3	-	-		V	-		
	146A2	3084	6507					
	137C2	V	L					**6507**
	132A2	V	-					
	146C	-						**?**
	147A1	-						
	18C2	3548	3189					
BLISTER	**101A**	L	V					**3548**
	149C5	L	V					
BLISTER + PATHERN DEFFECTS	**77A**	1491	3638	3138	6965			
	82A2	SL	V	V	V			**1491**
	119D2	SL	-	-	-			

113B1	420	3189	**420/3189**
136B1	L	L	
66B	5869		**?**
127C4	-		

The complementation groups are classified by its phenotype (First column) and separated by double lines. First, one allele representing the complementation group was crossed with the set of 36 deficiencies covering the majority of the 2L arm (upper mutant of each complementation group shown in the second column). When this allele failed to complement one or several deficiencies (complementation with deficiencies columns), we crossed all the other alleles of the complementation group with these deficiencies. Only the cases in which more than one allele failed to complement with one particular deficiency were taken as a probe of the inclusion of the complementation group in the interval covered by this deficiency (right column, "RESULT").

TABLE S2

Results of the mapping of complementation groups formed by one single allele

A) MUTANT	B) DEFICIENCY
LETHAL OVER 1 DEFICIENCY	
14B1	8674
24A	167
24C	2414
27C2	3189
29A2	7144
37C	781
62B1	4955
67A1	6999
78B	7144
88A2	167
89B2	3138
93A2/93A6	6999
95C4	4955
96C1	2583
101B1	1491
110B5	167
111C6	8674
128C3	167
131B2	5330
136B2/136B3	6965
139B	490
173B5	167
178B	420
179B3	7142
180A1	3189
185A2	2583
190A1	781
195A	**420/3189**

A) MUTANT	B) DEFICIENCY		
LETHAL OVER 2 DEFICIENCIES			
29C2	3084	**2982**	**556/1045**
41B	9270	3189	
46B4	3084	9270	
46B5	6648	1045	
50B2	6648	490	
75B5	3548	167	
80B2/80B3	3548	6648	
89B4	90	490	
127C3	3084	90	
132A1	2414	4955	
149C	3079	1491	
157B3	1567	5864	
LETHAL OVER 3 DEFICIENCIES			
106D5	3138	2583	**3189/167**
111B4	6338	2414	4955
116C1	3084	9270	3344
130D1	7497	781	**1491/2583**
LETHAL OVER 6 DEFICIENCIES			
141C5	3638	5330	3079
	2583	3189	**3138/6999**
VIABLE			
29D1	**68B**	**92C2**	**106B3**
111B1	**119D5**	**181B**	**130C1**

The alleles (columns A) are classified as failing to complement only one deficiency (left column), or more than one deficiencies (right columns). The 420 and 3189 deficiencies overlap, and therefore we assume that the mutant (195A) maps to the region of overlap. The alleles complementing all deficiencies are shown to the bottom right under the heading "VIABLE".